3D atom probe tomography of swift heavy ion irradiated multilayers

J. Juraszek, A. Grenier, J. Teillet, E. Cadel, N. Tiercelin, I. Monnet, M. Toulemonde

Atom probe tomography of swift ion irradiated multilayers

J. Juraszek [a,*], A. Grenier [a], J. Teillet [a], E. Cadel [a], N. Tiercelin [b], I. Monnet [c] and M. Toulemonde [c]

[a] *Université de Rouen, GPM UMR 6634 CNRS, BP12 F-76801 Saint-Etienne du Rouvray, France*

[b] *LEMAC-IEMN, DOAE UMR CNRS 8520, BP 69, F-59652 Villeneuve d'Ascq, France*

[c] *CIMAP-CIRIL, BP 5133 F-14070 Caen Cedex 5, France*

Abstract

Nanometer scale layered systems are well suited to investigate atomic transport processes induced by high-energy electronic excitations in materials, through the characterization of the interface transformation. In this study, we used the atom probe technique to determine the distribution of the different elements in a (amorphous-Fe_2Tb 5 nm/hcp-Co 3 nm)$_{20}$ multilayer before and after irradiation with Pb ions in the electronic stopping power regime. Atom probe tomography is based on reconstruction of a small volume of a sharp tip evaporated by field effect. It has unique capabilities to characterize internal interfaces and layer chemistry with sub-nanometer scale resolution in three dimensions. Depth composition profiles and 3D element mapping have been determined, evidencing for asymmetric interfaces in the as-deposited sample, and very efficient Fe-Co intermixing after irradiation at the fluence 7×10^{12} ion cm^{-2}. Estimation of effective atomic diffusion coefficients

after irradiation suggests that mixing results from interdiffusion in a molten track across the interface in agreement with the thermal spike model.

Key words: Ion beam mixing, atom probe tomography, multilayers, swift ion irradiation

PACS: 61.80.Jh, 68.55.Nq, 68.65.Ac, 42.30.Wb

---

1 Introduction

Irradiation with energetic ions is known to induce the formation of latent tracks in a wide range of materials, as the result of the huge energy density deposited locally along the ion path by electronic excitations. The study of the effects of swift ion irradiation on multilayered thin film is of growing interest from both fundamental and practical points of view. For the latter, ion beam mixing induced at the interfaces has been found as a very efficient tool to produce new materials and phases, and hence to modify in a control way the physical properties of the films [1]. From the fundamental point of view, nanometer scale layered systems are well suited to investigate the mechanisms allowing to convert high energy electronic excitations into atomic transport, through the fine scale characterization of the interface reactions [2,3].

For magnetic multilayers, ion irradiation is able to modify the direction of the perpendicular magnetic anisotropy of Fe/Tb multilayers [4–6], as well as the giant magneto-resistance of Fe/Cr multilayers [7,8]. Recently, we have found that the magnetostrictive properties of TbFe/Co multilayers can be greatly

* Corresponding author. Fax: +33 232 955 032
Email address: jean.juraszek@univ-rouen.fr (J. Juraszek).

improved after irradiation with swift ions [9]. In this system, the huge magnetostrictive susceptibility obtained by exchange coupling layers of TbFe with high magnetostriction and Co with high saturation magnetization allows new applications in the field of Magneto-Electro-Mechanical Systems (MEMS). The control of these properties by ion irradiation requires a detailed knowledge of local interfacial intermixing. While various techniques can be used to provide a concentration profile across an interface, only a few advanced methods of chemical analysis are suitable to obtain a local information at the nanometer scale. Among them, Secondary Ion Mass Spectroscopy (SIMS) and Rutherford Backscattering Spectroscopy (RBS), which have been widely used to study ion beam mixing [3]. Complementary techniques can also be used such as, conversion electron Mössbauer spectrometry with 0.5 nm thick ^{57}Fe marker layers, which has been demonstrated to be very efficient to characterize local ion-induced interface transformation [10,11]. Recently, a combination of x-ray reflectivity and fluorescence measurements was used to provide quantitative amount of mixing [12,13]. However, for all the above techniques, information is averaged over a large surface of the sample ($\geq$ 1 mm^2). In this report, we present a local chemical analysis of ion irradiation effects on TbFe/Co multilayers by the tomographic atom probe (TAP) technique. The TAP is an analytical microscope providing quantitative atomic scale 3D elemental mapping of chemical species in materials [14]. The technique, using a voltage pulse to field evaporate atoms from a sharp tip, was preliminary limited to metallic specimens, but the recent use of laser pulsing makes it possible analysis of poorly conducting materials [15]. The emergence of new focused ion beam methods has allowed to fabricate atom probe specimens from multilayered thin films. Analysis of multilayers can then provide a map of the composition of the layers and their interfaces, at the near atomic scale [16–18].

In a first part, the basic principle of the technique will be described, including special procedure to fabricate an atom probe specimen from multilayered thin films. Then we will present the analysis by TAP of the microstructure of the as-deposited multilayer and its modification after ion irradiation.

2 The tomographic atom probe

The atom probe is the combination of a field ion microscope, for which surface atoms are evaporated as ions by field effect, and a time of flight mass spectrometer allowing their identification. The specimen is prepared in the shape of a sharp tip (with apex < 100 nm radius), allowing the generation of a high electric field ($\simeq 10^6$ V m^{-1}) at the tip apex by applying a high voltage ($\simeq 10$ kV). By using high voltage (HV) pulses of about 20% of the standing voltage, ions can be evaporated from the specimen at a well defined time. The flight time of each evaporated ion can then be measured and used to calculate the mass-to-charge ratio and thus determine its chemical nature [19,20]. In the 3D atom probe, the gradually evaporated ions are projected on a two-dimentional sensitive detector. The analysis proceeds by continued removal and detection of individual ions, layer-by-layer through the material. The combination of two-dimensional hit positions and field evaporation sequence is thus used for the reconstruction of a three-dimensional image of the analyzed volume with near-atomic resolution.

This instrument provides the highest spatial resolution for a large analyzed volume, typically 25 nm by 25 nm by 50 nm, as compared to other microanalysis techniques: the depth resolution is better than 0.1 nm and that in lateral is a few thenths of nanometer, physically limited by ion-optical aberrations.

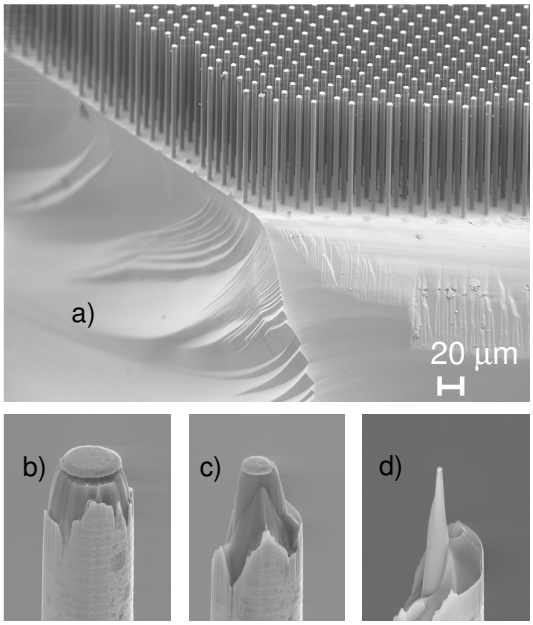

Fig. 1. FIB-based method to produce a sharp needle specimen by progressive annular milling of Si posts [from (a) to (d)].

Another advantage is its quantitavity: the concentration can be simply calculated from the number of ions of each kind of atoms collected and does not depend on cross section or ionisation efficiency [21]. Possible sources of errors in the interpretation of 3D images and local composition include possible mass overlap between some elements in the mass spectrum, statistical fluctuations due to sampling errors, preferential evaporation of low field species, and impact overlaps on the detectors [21]. With combination of recent developments in specimen preparation techniques by focused ion beam (FIB) [22,23] and TAP, it is possible to analyse thin films and multilayers [18,24]. Atom probe tomography is then an ideal technique to quantify the degree of atomic intermixing at the interface and within the individual layers because of its high spatial resolution. Not only does the concentration profile across an interface can be obtained, but also the morphology and rugosity of this interface.

3 Experimental

3.1 Deposition and ion irradiation of Tb-Fe/Co multilayers

Multilayers were deposited at room temperature by rf-sputtering of pure Co and composite $TbFe_2$ targets onto flat-topped cylindrical Si posts that were prepared by deep reactive ion etching for atom probe analysis, and onto flat Si wafers for conventional analyses. The multilayers involve twenty repetitions of ($TbFe_2$ 5 nm/Co 3 nm) bilayers, with Co as a starting layer. A 5 nm Ti capping layer was used for protection against oxidation. X-ray diffraction showed that Co layers are polycrystalline while FeTb layers are amorphous. Room temperature irradiations of pristine samples (planar and post substrates) were then performed with 450 MeV Pb ions at the fluence $7{\times}10^{12}$ ion cm^{-2} under normal incidence at the medium energy line of the GANIL accelerator. The flux was limited to 3×10^8 ion cm^{-2} s^{-1} in order to avoid heating during irradiation. From SRIM calculations [25], the values of the electronic (nuclear) stopping power are 60 (0.27) keV nm^{-1} for Co and 44 (0.20) keV nm^{-1} for FeTb, respectively. Nuclear energy loss has then no significant effect at the fluence used here, and interfacial reactions are predominantly due to electronic energy loss. The projected range of the ions being 100 times higher than the multilayer thickness, they get buried deeply in Si substrate. Therefore the electronic energy loss can be considered as almost constant throughout the multilayer.

3.2 Tip fabrication

The tip preparation procedure is based on annular FIB milling of the samples deposited onto flat-topped Si posts, as described in details in Refs. [26,27]. A Cr capping layer is deposited prior to the milling in order to limit sample preparation damage. The posts are removed from the wafer and one of them is fixed to an ultra fine stainless steel pin with an electrically conducting silver epoxy. Milling is then performed in sequential concentric circles with a 30 keV Ga ion beam, sharpening progressively the apex of the sample. At the end of milling, the apex radius is about 10 nm. An example of an atom probe specimen produced with the described method is shown in Fig. 1. Gallium implantation can also damage the sample by producing intermixing of the layers or amorphization at the top and near the outer hedge of the tip [26]. The range of Ga ions is about 20 nm but it can produce ion beam mixing due to collision cascades at a distance over 30 nm from the tip surface. To avoid such effects, we will only present atom probe analysis data of the center of the multilayers by selecting a reconstruction volume far from the Ga ion implantation zone.

4 Results and discussion

In order to provide 3D data with an absolute length scale along the depth direction, the bilayer thicknesses of the as-deposited and ion irradiated samples elaborated on conventional Si substrates were measured by x-ray Reflectometry (XRR). The least-square fitting of experimental data has been performed using SimulReflect software. For the as-deposited sample, the modulation of

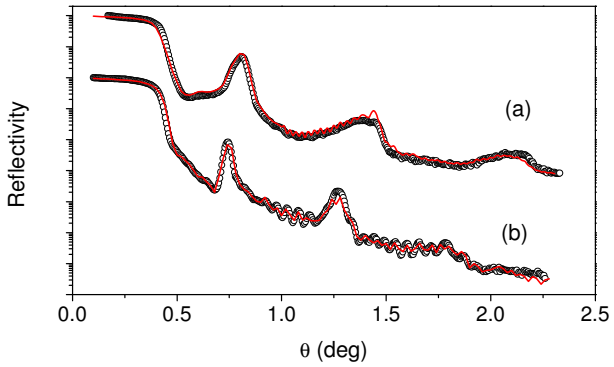

Fig. 2. Experimental and fitted x-ray reflectometry patterns of the (Tb-Fe 5 nm/Co 3 nm) multilayer: asdeposited (a) and irradiated with Pb ions at the fluence 7×10^{12} ion cm^{-2} (b).

the intensity above the critical angle is in agreement with the modulation of composition inside the multilayer [Fig. 2(a)]. It can be seen that for the irradiated sample, a modulation of composition still exists in the sample but the position and width of the peaks have slightly changed, evidencing for a modification of the layered structure [Fig. 2(b)]. The average values of the multilayer period, i.e., the thickness of the Tb-Fe/Co bilayers, deduced from the fit are 7.7 ($\pm$0.2) nm and 8.8 ($\pm$0.2) nm, respectively, for the as-deposited and ion irradiated specimens. These values have been used to calibrate precisely the depth scale of the TAP data.

In Fig. 3 (a), the atomic reconstruction of a middle part of the multilayer is shown for the as-deposited state. Each elemental dot is the calculated image of a single atom. Measurements were carried out in an energy-compensated optical tomographic atom probe (ECOTAP) [28], with a vacuum of $\simeq 10^{-10}$ Pa, at a pulse rate of 2 kHz and a specimen temperature of 80 K. The number of collected atoms in this volume is about 10^5, corresponding to a 32 nm thick stacking. The results show a well-defined sequence of Co and Tb-Fe layers,

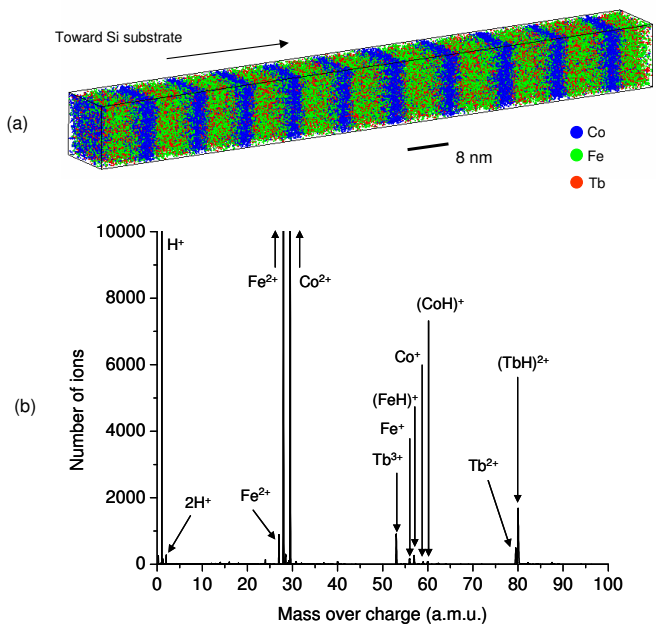

Fig. 3. 3D reconstruction of the distribution of Fe, Tb and Co atoms (a) and corresponding mass spectrum (b) for the as-deposited Tb-Fe/Co multilayer.

with a thickness ratio of about 0.6, in good agreement with the nominal one. A precise analysis of the atom distribution evidences for planar interfaces on the lateral length scale of the measurement. From the mass spectrum plotted in Fig. 3(b), it can be seen that each peaks are clearly separated, so that the mass resolution is high enough to provide accurate composition determination. It should be noted that no significant Ga was detected in this analyzed region, indicating that the layered structure was not affected by the tip preparation process.

A higher magnification of the reconstruction of the as-deposited multilayer is shown in Fig. 4(a). The apparent density inside the FeTb layers is quite homogeneous. Some diffusion of Co atoms inside the FeTb layer can be observed. It should be noted that no atomic planes were observed in the Co layers, despite their cristallinity evidenced by x-ray diffraction (XRD). Because of the ion trajectory aberrations limiting the lateral resolution, the chance to observe such

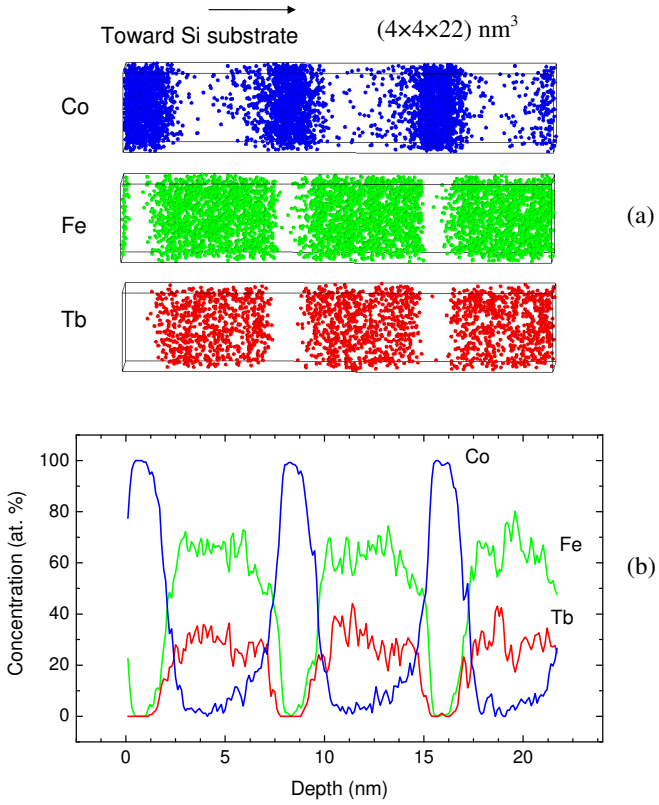

Fig. 4. 3D reconstruction of the distribution of Fe, Tb and Co atoms (a) and corresponding concentration profile (b) in a selected volume of the as-deposited Tb-Fe/Co multilayer.

atomic planes for strongly textured specimens is very weak if there is a small misalignment of the analysis direction with respect to the crystallographic orientation of Co grains.

The orientation of the volume was chosen in order to obtain a composition profile perpendicular to the plane of the layers, as plotted in Fig. 4(b). The small lateral dimensions of the volume increase the statistical fluctuations but minimise the averaging out of fine scale variations, allowing determination of chemical mixing independant of interface roughness. At both interfaces of the as-deposited multilayer, an interfacial solid solution between Co, Fe and Tb is observed. However the width of the intermixed zone is different according to

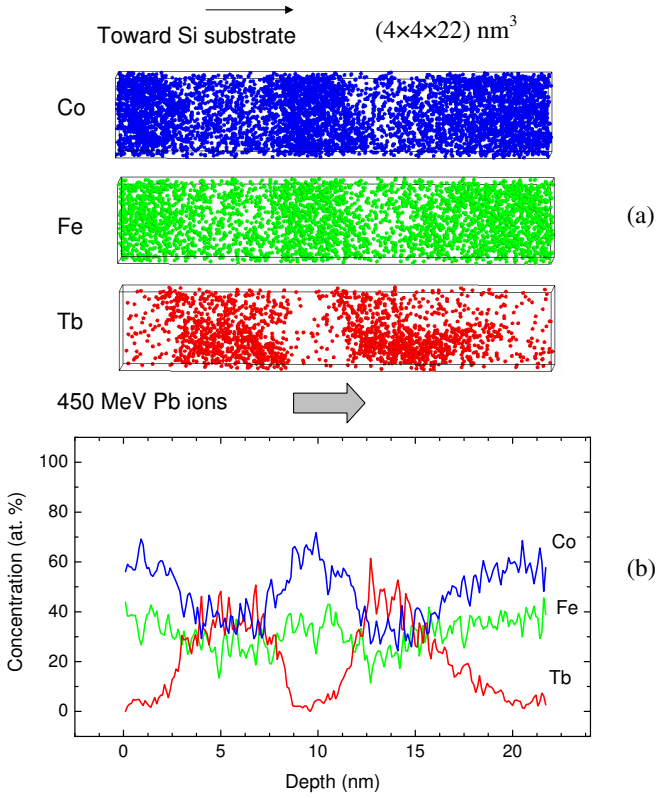

Fig. 5. 3D reconstruction of the distribution of Fe, Tb and Co atoms (a) and corresponding concentration profile (b) in a selected volume of the Tb-Fe/Co multilayer irradiated with Pb ions at the fluence 7×10^{12} ion cm^{-2}.

the position of the interface in the stack. Interface width of 1 ($\pm$0.3) nm and 3 ($\pm$0.4) nm for the TbFe-on-Co and Co-on-TbFe interfaces, respectively, were measured on the experimental data. So, cobalt atoms penetrate more deeply inside the Tb-Fe layers when they are deposited on top of them, rather than when the Fe and Tb atoms are simultaneously deposited onto the Co layers. A measurement of the concentration at the center of the Tb-Fe layers yields 33% Tb, 66% Fe, in well agreement with the nominal target composition. The center of the cobalt layers is quite pure.

The TAP analysis of the multilayer irradiated with Pb ions at the fluence 7×10^{12} is shown in Fig. 5. Element mapping, as well as, concentration pro-

files of Co and Fe indicate that a quasi-complete intermixing between these elements has occured during irradiation of the multilayer. The Fe composition becomes quite homogeneous in the whole part of the irradiated sample, but a slight modulation of composition still exists for cobalt. In the initially pure Co, the average composition becomes Co-35($\pm$5)% Fe after irradiation. Such interdiffusion effects have also strongly modified the composition of the amorphous Tb-Fe layers, which become layers of a Co-rich Tb-Fe-Co alloy. Modification of the average width of Tb layers doesn't exceed 1 nm, indicating that transport of Tb atoms induced by swift heavy ion irradiation is much lower than that of Fe and Co atoms. We emphasize that, as for the non-irradiated sample, detection of Ga ions in this selected volume of the Pb ion-irradiated multilayer is negligeable. The observed intermixing can then be solely attributed to the effects of swift ion irradiation.

The modification of the layers composition from Tb-Fe/Co to Tb-Fe-Co/Fe-Co is in agreement with the change of the magnetostrictive properties after irradiation observed on similar multilayered system [9]. Strong increase of the saturation magnetization and magnetoelastic coefficient have been evidenced below a critical fluence $\phi_c \simeq 1.6 \times 10^{12}$ ion cm^{-2}, followed by a saturation regime for higher fluences. We show here that enhancement of these magnetic properties is due to a very efficient mixing between Fe and Co atoms at the interfaces. In addition, the quasi-complete Fe-Co intermixing obtained at the fluence 7×10^{12} ion cm^{-2} agrees with the saturation effects obtained for fluences above ϕ_c. Finally, the remaining layered structure evidenced at the high studied fluence agrees with the excellent soft magnetic properties of the irradiated samples.

Mixing at the interface between layers of different materials in the electronic

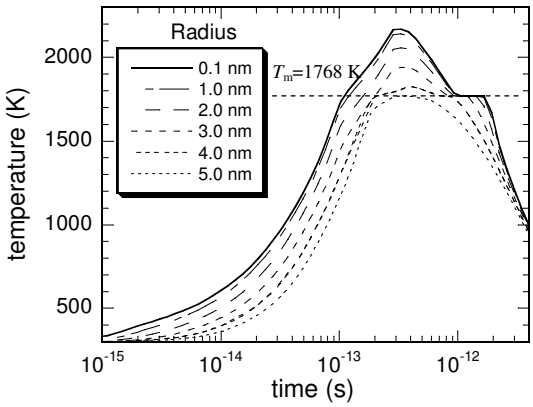

Fig. 6. Evolution of the lattice temperature versus time for various radial distances in bulk Co irradiated with Pb ions at room temperature as calculated using thermal spike simulations. T_m is the melting temperature of bulk Co.

stopping regime usually occurs above an electronic stopping power threshold. The thermal spike model has been succesfully employed in oxide ceramics [29,30], as well as metallic systems [29,31,32], to explain mixing by considering interdiffusion effects in a molten ion track. The threshold is then related the electronic energy density which should be high enough to generate a transient molten phase at both sides of the interface [31,29,33].

Assuming that mixing results from a transient molten phase inside the ion track, the fluence $\phi_c = 1.6 \times 10^{12}$ ion cm^{-2} from which saturation effects of magnetic properties have been observed, corresponds to a complete irradiation of the whole sample surface for the first time. The subsequent studied fluence $\phi_f = 7 \times 10^{12}$ ion cm^{-2} would then correspond to $n = \phi_f/\phi_c \simeq 4$ full overlaps of tracks. The present ϕ_c value is close to that reported in the case of molten tracks in thin Fe films, implying a similar track diameter [34]. From the obtained modifications of the composition profiles, it is then possible to measure diffusion length of a specific element from the interface broadening and thus, to estimate its effective atomic diffusion constant based on the assumption of

transient thermal mixing. Interface broadening caused by the impact of one single ion is given by $\Delta l = 2\sqrt{Dt}$, where D and t are the diffusion constant and diffusion time, respectively. The evolution of the bulk Co lattice temperature with time for different radial distances around the ion path of 450 MeV Pb ions, as calculated using the thermal spike model [35,36], is shown in Fig. 6. It can be seen that the temperature of the lattice remains above the melting temperature for a duration of about $t_m = 1$ ps at a radius of 4 nm. Therefore, the diffusion time for the observed changes in depth distribution of Co in Tb-Fe and Fe in Co at the fluence ϕ_f is equal to nt_m. The obtained effective diffusion constants of about $10^{-7} - 10^{-8}$ m^2s^{-1} are in agreement with a diffusion process in liquid phase rather than solid state diffusion. Such results support the assumption that the strong Fe-Co interdiffusion evidenced at the interfaces by TAP occurs during mixing in a molten track.

5 Conclusion

Atom probe technique has been used to study the evolution of the interface morphology and chemical intermixing in a TbFe/Co multilayer irradiated with 400 MeV Pb ions. The 3D element mapping shows that the layered structure is strongly modified after irradiation at the fluence 7×10^{12} ion cm^2 as the result of significant Fe-Co interdiffusion at the interfaces between Tb-Fe and Co layers. The thermal spike model is well suited to explain such strong interdifusion at a rather low fluence by assuming enhanced diffusion in a transient melt phase along the ion trajectory. Work is in progress to analyse samples irradiated at a fluence close to the critical fluence for first overlapping of the tracks, in order to study mixing induced in the wake of a nearly single ion. To-

mographic atom probe is demonstrated to be a very powerful technique to investigate at the subnanometer scale swift irradiation effects in nanostructured materials, and more particularly, to study ion beam mixing in multilayers.

Acknowledgments

The authors are grateful to the staff of CIMAP for the assistance during the irradiation experiments at GANIL. This work was funded by the european INTERREG IIIA program n°198 and by The Ministère de l'Enseignement Supérieur et de la Recherche.

References

[1] W. Bolse, Surface & Coatings Technology 158 (2002) 1–7.

[2] W. Bolse, B. Schattat, Nuclear Instruments & Methods In Physics Research Section B-Beam Interactions With Materials And Atoms 190 (2002) 173–176.

[3] W. Bolse, B. Schattat, Nuclear Instruments & Methods In Physics Research Section B-Beam Interactions With Materials And Atoms 209 (2003) 32–40.

[4] J. Teillet, F. Richomme, A. Fnidiki, M. Toulemonde, Physical Review B 55 (17) (1997) 11560–11568.

[5] A. Gupta, A. Paul, R. Gupta, D. K. Avasthi, G. Principi, Journal Of Physics-Condensed Matter 10 (43) (1998) 9669–9680.

[6] J. Juraszek, A. Fnidiki, J. Teillet, F. Richomme, N. H. Duc, M. Toulemonde, W. Keune, Applied Physics Letters 74 (16) (1999) 2378–2380.

[7] M. Kac, M. Toulemonde, J. Jaworski, J. Juraszek, R. Kruk, S. Protsenko, V. Tokman, M. Marszalek, Vacuum 78 (2-4) (2005) 661–665.

[8] A. Gupta, D. Kumar, Nuclear Instruments & Methods In Physics Research Section B-Beam Interactions With Materials And Atoms 244 (1) (2006) 202–205.

[9] J. Juraszek, A. Grenier, J. Teillet, N. Tiercelin, F. Petit, J. Ben Youssef, M. Toulemonde, Nuclear Instruments & Methods In Physics Research Section B-Beam Interactions With Materials And Atoms 245 (1) (2006) 157–160.

[10] J. Juraszek, A. Fnidiki, J. Teillet, M. Toulemonde, A. Michel, W. Keune, Physical Review B 61 (1) (2000) 12–15.

[11] J. Juraszek, J. Teillet, A. Fnidiki, M. Toulemonde, Hyperfine Interactions 156 (1) (2004) 615–621.

[12] A. Gupta, P. Rajput, A. Saraiya, V. R. Reddy, M. Gupta, S. Bernstorff, H. Amenitsch, Physical Review B 72 (7) (2005) 075436.

[13] P. Rajput, A. Gupta, V. R. Reddy, V. Sathe, D. K. Avasthi, Journal Of Physics-Condensed Matter 19 (3) (2007) 036221.

[14] D. Blavette, A. Bostel, J. M. Sarrau, B. Deconihout, A. Menand, Nature 363 (6428) (1993) 432–435.

[15] B. Gault, A. Menand, F. de Geuser, B. Deconihout, R. Danoix, Applied Physics Letters 88 (11) (2006) 114101.

[16] D. J. Larson, A. K. Petford-Long, A. Cerezo, G. D. W. Smith, Acta Materialia 47 (15-16) (1999) 4019–4024.

[17] J. Schleiwies, G. Schmitz, S. Heitmann, A. Hutten, Applied Physics Letters 78 (22) (2001) 3439–3441.

[18] A. Grenier, R. Larde, E. Cadel, F. Vurpillot, J. Juraszek, J. Teillet, N. Tiercelin, Journal Of Applied Physics 102 (3) (2007) 033912.

[19] D. Blavette, B. Deconihout, A. Bostel, J. M. Sarrau, M. Bouet, A. Menand, Review Of Scientific Instruments 64 (10) (1993) 2911–2919.

[20] T. F. Kelly, M. K. Miller, Review Of Scientific Instruments 78 (3) (2007) 031101.

[21] D. Blavette, B. Deconihout, S. Chambreland, A. Bostel, Ultramicroscopy 70 (3) (1998) 115–124.

[22] D. J. Larson, D. T. Foord, A. K. Petford-Long, T. C. Anthony, I. M. Rozdilsky, A. Cerezo, G. W. D. Smith, Ultramicroscopy 75 (3) (1998) 147–159.

[23] D. J. Larson, B. D. Wissman, R. L. Martens, R. J. Viellieux, T. F. Kelly, T. T. Gribb, H. F. Erskine, N. Tabat, Microscopy And Microanalysis 7 (1) (2001) 24–31.

[24] A. Cerezo, P. H. Clifton, S. Lozano-Perez, P. Panayi, G. Sha, G. D. W. Smith, Microscopy And Microanalysis 13 (6) (2007) 408–417.

[25] J. F. Ziegler, Srim-2003, Nuclear Instruments and Methods in Physics Research Section B: Beam Interactions with Materials and Atoms 219-220 (2004) 1027–1036.

[26] G. B. Thompson, M. K. Miller, H. L. Fraser, Ultramicroscopy 100 (1-2) (2004) 25–34.

[27] M. K. Miller, K. F. Russell, G. B. Thompson, Ultramicroscopy 102 (4) (2005) 287–298.

[28] E. Bemont, A. Bostel, M. Bouet, G. Da Costa, S. Chambreland, B. Deconihout, K. Hono, Ultramicroscopy 95 (1-4) (2003) 231–238.

[29] W. Bolse, Radiation Measurements 36 (1-6) (2003) 597–603.

[30] B. Schattat, W. Bolse, Nuclear Instruments and Methods in Physics Research Section B: Beam Interactions with Materials and Atoms 225 (1-2) (2004) 105–110.

[31] Z. G. Wang, C. Dufour, S. Euphrasie, M. Toulemonde, Nuclear Instruments and Methods in Physics Research Section B: Beam Interactions with Materials and Atoms 209 (2003) 194–199.

[32] S. K. Srivastava, D. K. Avasthi, W. Assmann, Z. G. Wang, H. Kucal, E. Jacquet, H. D. Carstanjen, M. Toulemonde, Physical Review B 71 (19) (2005) 193405.

[33] A. Chettah, Z. Wang, M. Kac, H. Kucal, A. Meftah, M. Toulemonde, Nuclear Instruments and Methods in Physics Research Section B: Beam Interactions with Materials and Atoms 245 (1) (2006) 150–156.

[34] D. K. Avasthi, W. Assmann, A. Tripathi, S. K. Srivastava, S. Ghosh, F. Gruner, M. Toulemonde, Physical Review B 68 (15) (2003) 153106.

[35] M. Toulemonde, C. Dufour, E. Paumier, Phys. Rev. B 46 (22) (1992) 14362–14369.

[36] Z. G. Wang, C. Dufour, E. Paumier, M. Toulemonde, Journal Of Physics-Condensed Matter 6 (34) (1994) 6733–6750.